R-99-01

Geosphere Performance Indices:

Comparative measures for site selection and safety assesment of deep waste repositories

Vladimir Cvetkovic
Division of Water Resources Engineering
Royal Institute of Technology

Jan-Olof Selroos
Svensk Kärnbränslehantering AB

January 1999

Svensk Kärnbränslehantering AB
Swedish Nuclear Fuel
and Waste Management Co
Box 5864
SE-102 40 Stockholm Sweden
Tel 08-459 84 00
+46 8 459 84 00
Fax 08-661 57 19
+46 8 661 57 19

ISSN 1402-3091
SKB Rapport R-99-01

Geosphere Performance Indices:

Comparative measures for site selection and safety assessment of deep waste repositories

Vladimir Cvetkovic
Division of Water Resources Engineering
Royal Institute of Technology

Jan-Olof Selroos
Svensk Kärnbränslehantering AB

January 1999

Keywords: Geosphere retention, performance assessment, site selection, stochastic transport modelling

Abstract

The concept of *Geosphere Performance Indices* (GPIs) is proposed. The "performance" refers to the geosphere's capacity to retain/contain radionuclides in the event of their accidental release at some point in time. The GPIs are based on the Lagrangian stochastic-analytical framework for transport in the subsurface and are believed to render useful tools in performance assessment studies in general and in the site selection process in particular. A few advantages of the GPIs are: their transparency, low computational and the fact that additional data in a site selection programme can be incorporated in an iterative manner. Illustration examples indicate that the probability of the GPIs depends strongly on the dimensionless system parameters eB, aB and $dB^{1/2}T^{-1}$. It is proposed that the derived framework is further elaborated and applied for realistic geosphere cases.

Contents

1 Introduction **1**

2 Scenarios and criteria **3**

3 Theory **10**

4 Radionuclide discharge **13**

4.1 Scenario A: Pulse release 13

4.2 Scenario B: Continuous release 14

5 Geosphere performance indices (GPIs) **16**

5.1 Containment index 16

5.2 Arrival time indices 16

5.3 Dilution indices 18

5.4 Controlling parameters 19

6 Statistical formulation of GPIs **20**

7 Illustration examples **21**

7.1 Containment index 21

7.2 Mean arrival time index 23

7.3 Dilution index 25

8 Summary **26**

9 Appendix A: Laplace transform solutions **28**

10 Appendix B: A few results from probability theory **29**

1 Introduction

As part of the site selection program, different geological sites are to be considered and compared, using various criteria for site suitability. One such criteria is the potential of a site to contain radionuclides which depends on the combined physical and chemical properties of a given radionuclide and geological formation. Assessing the "performance" of geological media as a barrier for radionuclides is an integral part of the performance and safety assessment of deep nuclear waste repositories.

Recently the Swedish government and pertinent authorities have issued recommendations and specifications (Miljödepartmenetet, 1996; SKI, 1996) where a need for clear discrimination criteria between different potential sites for a deep-rock nuclear waste repository is identified. Furthermore, the government places a burden on SKB to clearly state and discuss those factors that actaully will govern the choice of a site, and to discuss how the criteria will be quantified. Thus, there is an obvious need for clear and comprehensive criteria and for a quantitative methodology for assessing site suitability as a consequence of current regulatory demands.

The potential of a particular site (geological medium) to contain radionuclides is usually assessed with a Performance Assessment (PA) analysis where the impact of the repository on the biosphere and man is evaluated. SKB has traditionally used a fairly complex numerical model chain for PA analyses (SKB, 1992). These type of models could in principle also be used to compare different sites when all data needed for the models are available; this is in fact to a certain extent pursued in the ongoing safety assessment SR 97 where three sites are compared in terms of overall safety. However, site selection and calculation of radionuclide doses in the biosphere do not necessarily have to be identical tasks. A project aiming at identifying key issues related to performance of geological barriers has been carried out (Olsson, 1995). Furthermore, a project aiming at identifying the most important parameters for the choice between different sites has recently been initiated at SKB (Andersson et al., 1997). In this project, not only parameters directly related to traditional PA analyses are identified, but also parameters related to repository construction, general geohydrologic understanding and other environmental issues are incorporated. The manner in which all the information is to be integrated and how the criteria are to be set for making the actual choices have not yet been fully addressed. It may be concluded, however, that fairly simple methodologies for comparing and screening between sites as new data emerges, without performing full PA analyses, are required. The effort of full PA analyses is simply too high. Ideas from the type of vulnerability analyses used in other groundwater related fields may here serve as a starting point on how

vulnerability/safety of a given site can be assessed in a simplified manner.

In this report we propose the concept of "geosphere performance indices" as comparative measures for the potential of a geological formation to act as a barrier for, or to contain, radionuclides. Our approach derives from the theoretical framework for safety assessment based on the Lagrangian approach by Selroos (1997a,b) and from recent advances in modelling solute migration in rock fractures (Selroos and Cvetkovic 1997; Cvetkovic et al. 1998). The objective is to arrive at a simple, yet useful, tool which at least partially can be used in the regulatory context outlined above. An important limitation of the approach is that we study the performance of the geosphere only from a pure radionuclide retention potential perspective. We ackwnoledge that other aspects such as the suitability of the geosphere for construction purposes and the long term stability in mechanical and chemical conditions (SKB, 1995) may be equally important. However, these issues are not addressed here. Compared to classical vulnerability assessment based on parameter classification, the proposed methodology differs by the fact that the governing equations of the studied sytem are identified and solved. However, the result of the methodology is hoped to be equally transparent as those of vulnerability analyses. The main contribution of the present work is to offer simple criteria within a probabilistic methodology where the performance of different sites can be compared quantitatively given the uncertainty in the underlying processes. Thus, a methodology for decision making under uncertainty is presented.

2 Scenarios and criteria

The problem configuration is illustrated in Figure 1. We consider a hypothetical repository consistent with the KBS-3 concept, located deep in geological media. Hundreds of canisters have been placed in the rock and are spread over a considerable area/volume; a typical scale of the entire repository in the horizontal dimension is of the order $10^3 m$. On such a scale many canisters intersect fractures (that may be more or less sealed) with probability 1. Furthermore, given the number of canisters, failure of one or several of them is certain (probability 1), albeit the time, location and release conditions of the failure(s) are uncertain.

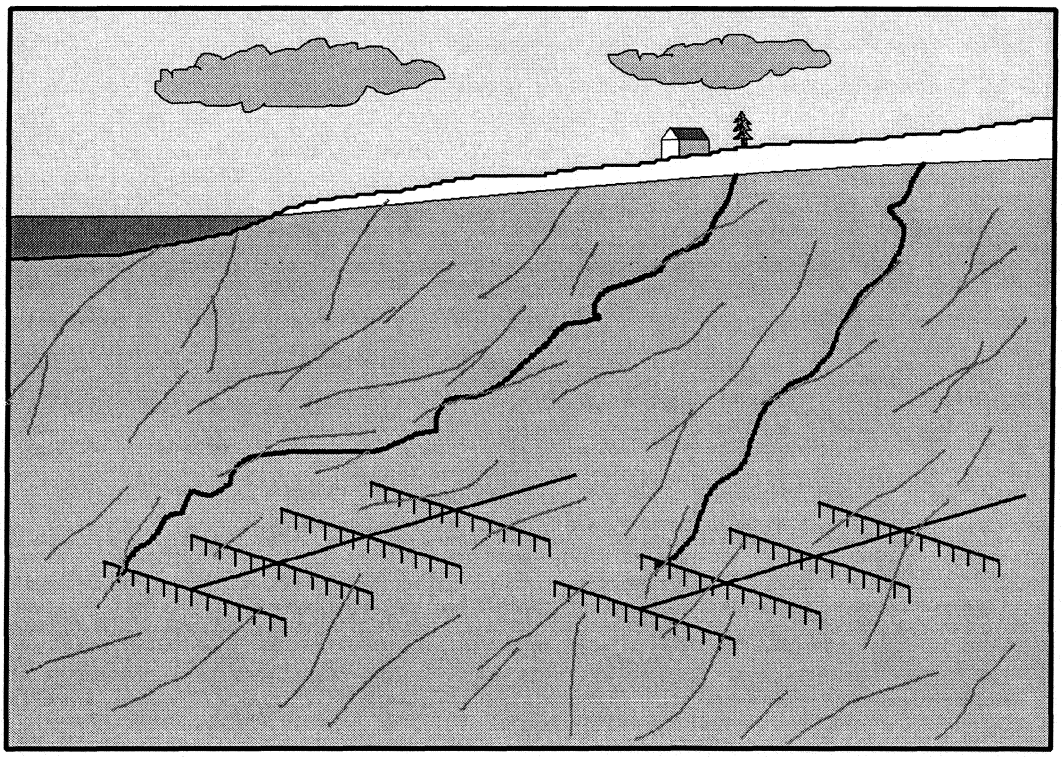

Figure 1: Problem configuration sketch.

Once released into the geological medium, radionuclides migrate toward the biosphere due

to groundwater movement. Diffusion and sorption of radionuclides into the rock retard their migration, at best allowing time for complete decay; in such a case, the geosphere is an ideal barrier. Short of full decay, some mass will eventually be released into the bioshpere; in such a case, the geological medium is only a partial barrier. The degree to which a geological site constitutes a barrier for any released radionuclide depends on the site's physical and chemical properties.

The release of radionuclides is hypothesized to take place from a single canister on a relatively small scale of the order $< 10^0 m$. Given the small injection scale, we shall assume that the radionuclides migrate along a *single* flow path (streamtube) which extends through intersecting conducting features. In other words, released radionuclides are transported by advection, and are *divisible* only by mass transfer. The conducting features are essentially two-dimensional fractures which for discussion purposes we may consider as predominantly planar. Clearly part of the radionuclide particles will disperse for instance at fracture intersections, entering different fractures and flow paths. However, we assume that one of these flow paths is dominant in advecting most of the radionuclide particles from the failed canister to the biosphere (e.g., Rasmuson and Neretnieks, 1984; Selroos 1997a,b). A segment of a random advection flow path through rock fractures is illustrated in Figure 2.

Let m_0 denote the mass of any radionuclide released at time $t = t_0$ from a canister at the location $\mathbf{x} = \mathbf{x}_c$. Note that we shall refer to m_0 as mass although the dimensions of m_0 may be mass or energy. Also note that m_0 is not the mass deposited, but rather the mass present at the time of release. Eventhough only single radionuclides are addressed in the present context, the methodology may be extended to incorporate radionuclide decay chains.

Two basic scenarios are considered, referred to as scenario (A) and (B). In scenario (A), the mass m_0 is released instantaneously (as a pulse), i.e. over a relatively short period of time. In scenario (B), the m_0 is released over a long period of time i.e. continuously at a constant intrinsic rate q_0 $[MT^{-1}]$. The actual release rate at the injection point is $q_0 \mathrm{e}^{-\lambda(t-t_0)}$ due to decay, where λ $[T^{-1}]$ is the decay rate for a given radionuclide. The total mass released from the canister is m_0, computed for scenario B as

$$m_0 = q_0 \int_{t_0}^{\infty} \mathrm{e}^{-\lambda(t-t_0)}\, dt = \frac{q_0}{\lambda}$$

The location $\mathbf{x}_c$ and time of release t_0, are unknown parameters which can never be determined. Consequently, the parameters m_0 and q_0 are uncertain. Hence we set our frame of reference at $\mathbf{x}_c$ and t_0 with $t_0 = \mathbf{x}_c = 0$, and use m_0 or q_0 as normalization parameters.

If the geosphere is only a partial barrier for the released radionuclides, the breakthrough at the geosphere-biosphere interface provides the release history into the biosphere. Figure 3

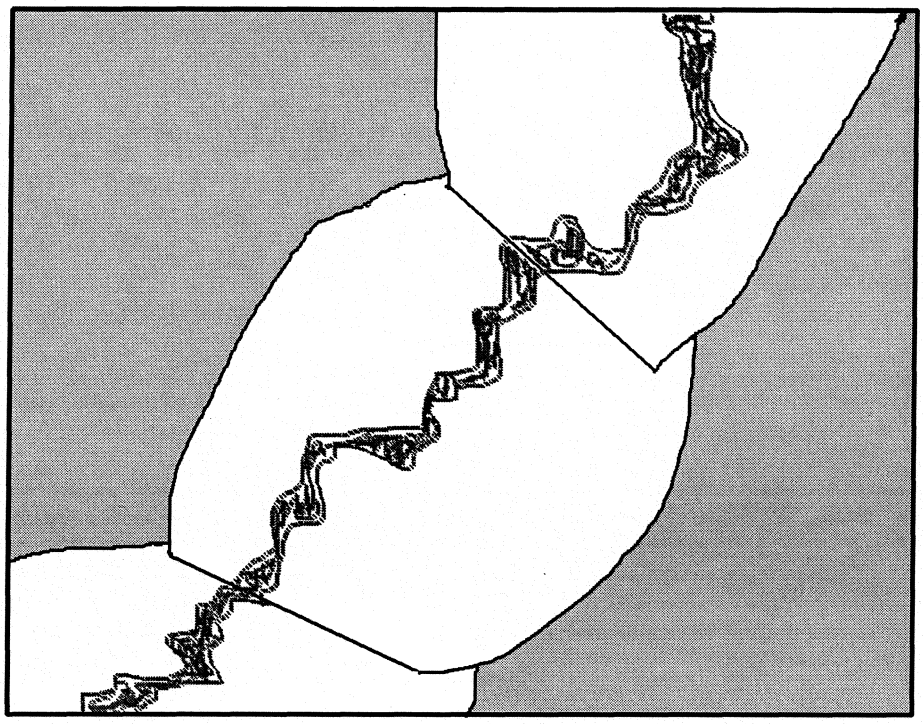

Figure 2: Configuration sketch of radionuclide transport through a series of interconnected fractures.

is an illustration sketch of the breakthrough for scenarios (A) and (B), for two different cases. Consider first case 1. If hydrodynamic dispersion and mass transfer processes (diffusion and sorption) are neglected, a pulse of diminished strength arrives with groundwater in scenario (A) (Figure 3a), whereas in scenario (B) the breakthrough exhibits exponential tailing due to decay (Figure 3b). If the mass transfer processes are accounted for, the breakthrough for scenario (A) is dispersed (even in the absense of hydrodynamic dispersion) (Figure 3a), whereas for scenario (B) the dispersion is considerably enhanced by the continuous release (Figure 3b).

The hypothetical discharge of radionuclides into the biosphere in the two scenarios discussed above, will generally differ between different sites, for both deterministic and statisti-

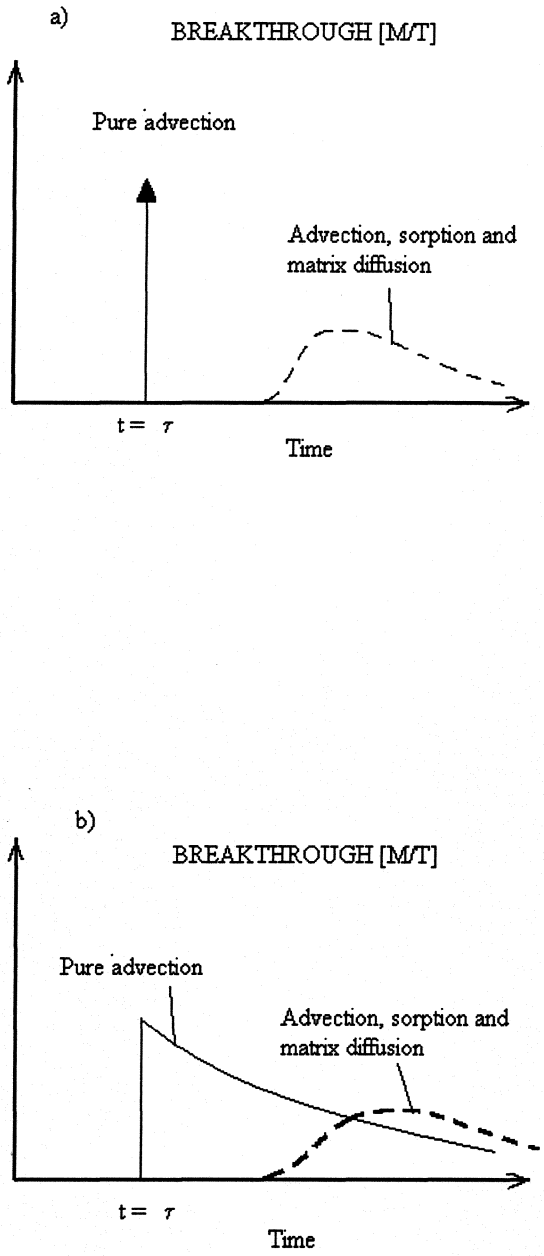

Figure 3: Qualitative behavior of the radionuclide breakthrough into the biosphere for two considered scenarios: (a) pulse release (scenario (A)), (b) for continuous release (scenario (B)).

cal reasons. In particular, if we consider two geological sites, the parameters which control mass transfer processes and can be determined in the laboratory from samples, will be different (deterministic reasons). Furthermore, hypothetical breakthrough curves at different sites will differ due to the natural heterogeneity of flow and mass transfer properties of geological media which can be accounted for only statistically (statistical reasons).

In this report, we propose probabilitstic measures of geosphere's potential to act as a barrier for specified radionuclides, referred to as *geosphere performance indices* (short GPIs). The GPIs are to be defined such that they can be compared between different sites, or used directly in the context of performance and safety assessment. The GPIs are obtained analytically; all used solutions are purely analytical and the statistics on the underlying parameters are obtained from the field (or alternatively from numerical simulations if field data is not available). In this study we shall hypothesize the statistical parameters for illustrative purposes. The mean values will be normalized with quantities that can in principle be determined for any given site.

We shall consider three classes of GPIs:

(i) Containment index This index estimates geosphere's potential at a given site to contain radionuclides; in particular, it quantifies the difference between m_0 and the total mass released into the biosphere either following scenario (A) or (B), normalized by m_0.

(ii) Arrival time indices These estimate the radionuclide time of arrival to the biosphere for either scenarios, for instance, the mean arrival time, the arrival time of the peak, fractional time of arrival such as first arrival, etc., suitably normalized.

(iii) Dilution indices These estimate the magnitude of dilution due to dispersive effects by quantifying the time during which a radionuclide is discharged into the biosphere, for instance, the second temporal moment (variance) of the breakthrough curves, the magnitude of the peak, etc., suitably normalized.

In order to establish GPIs as quantitative, comparative measures, we follow several criteria that are listed below. GPIs are required to be:

accessible ; the GPIs have to be formulated such that they depend only on information (or parameters) that can be measured/characterized *here* and *now*, i.e. within the site-selection and site-characterization programs. Thus GPIs cannot depend on the unknown

quantities such as time and/or location of failure, the total mass or mass rate of radionuclide release, or the potential effects of radionuclides in the biosphere.

conservative ; the unavoidable simplifications in modelling radionuclide migration through geological media over large temporal and spatial scales should (to our best knowledge) be conservative.

realistic ; the GPIs have to account for what at the present state of knowledge are considered as the most dominant physical and chemical processes, at the same time complying with the preceding criterion ("conservative"). Furthermore, any realistic comparative measure has to be ultimately a *statistical* one, given the scales involved and heterogeneity of geologcal media.

transparent ; models of the key physical and chemical processes used for computing GPIs have to be relatively simple and transparent, such that a typical engineer (expert or from the public) can understand what is involved in the computations.

reproducible ; the computations of GPIs used in the site-selection and characterization programs must be relatively easy to reproduce by a typical engineer (expert or from the public). Using readily accessible software packages such as Maple, Mathematica or Mathcad, for instance, an engineer should be able to reproduce computations within a reasonable time frame (say a week). In practice, this implies that the computations are based on analytical expressions.

The use of analytical solutions, indices, or back-of-the-envelope-calculations in order to assess the geosphere barrier function has previously been employed in e.g. the Cristallin-1 Safety Assessment report (Nagra, 1994). To our knowledge, however, analytical-stochastic indices have not been presented before in the context of nuclear waste repositories. It is furthermore noted that the so-called 'total transport resistance' or F-ratio used in several performance assessment studies, e.g. TVO-92 (Vieno et al., 1992) and SITE-94 (SKI, 1997), may be considered as a type of performance index (specifically containment indices) for the geosphere. However, the use of a 'flow wetted surface' in these formulations is not conceptually well defined. Moreover, probabilistic results are only obtained using numerical simulations in SITE-94; in TVO-92 only deterministic calculations were performed.

In §3 we provide the theoretical basis for the stochastic-analytical GPIs. In §4 we provide general solutions that will be used for defining the GPIs, and in §5 the definitions are given. In §6 we show how the statistics of the GPIs can be computed. In §7 we discuss how the GPIs

can be related to site characterization programs, and provide illustration examples on how the GPIs can be used in the context of site-selection.

3 Theory

The flow path is a three-dimensional entity that essentially consists of segments set in two-dimensional planar features (Figure 2). We introduce an intrinsic coordinate system with unit vectors ($\mathbf{n}_w, \mathbf{n}_s, \mathbf{n}_b$), where s is the intrinsic coordinate defined as the flow path length; $s = 0$ is the release point. The vector $\mathbf{n}_b$ is (locally) orthogonal to the fracture, and thus in the direction of the fracture aperture, $2b$ (b is the half-aperture). The advection velocity,$\mathbf{V}$, is parallel to $\mathbf{n}_s$, i.e. $V = |\mathbf{V}| = \mathbf{V} \cdot \mathbf{n}_s$, and $\mathbf{n}_w$, is locally orthogonal to $\mathbf{n}_s$ and $\mathbf{n}_b$, approximately being in the direction of the flow path width. The quantities ($\mathbf{n}_w, \mathbf{n}_s, \mathbf{n}_b$) and b and $\mathbf{V}$ are all Lagrangian, i.e. functions of the intrinsic coordinate s.

We denote by C_f $[ML^{-1}]$ the radionuclide (tracer) concentration in fractures (mobile), and by C_m $[ML^{-1}]$ the tracer concentration in the rock matrix (immobile), where C_m is defined per unit pore water; the concentrations are defined as one-dimensional along s for a flow path set in three-dimensional space. The mass balance equations are written along s and n_b (Figure 2) as

$$\frac{\partial C_f}{\partial t} + \frac{\partial q_f}{\partial s} = \psi_f \tag{1}$$

$$\frac{\partial C_m}{\partial t} + \frac{\partial q_m}{\partial n_b} = \psi_m \tag{2}$$

where ψ_f and ψ_m are source terms in the "fracture" (mobile fluid) and the rock "matrix" (immobile fluid/solid), respectively, with dimensions $[MT^{-1}L^{-1}]$; these depend on C_f, C_m, their gradients, etc., and on a set of parameters that control the mass transfer and ultimately the retention of radionuclides. q_f and q_m are radionuclide fluxes in the fracture and the rock matrix, respectively, with dimensions $[MT^{-1}]$.

Transport by groundwater in the fractures is assumed to be by *advection* only, i.e. we neglect hydrodynamic dispersion along flow paths. Hence

$$q_f(s,t) = V(s)C_f(s,t) \tag{3}$$

Transport in the rock matrix is assumed to be by *diffusion* only, i.e. tracer movement in the rock matrix by fluid advection and hydrodynamic dispersion is neglected. Furthermore, we shall consider only the concentration gradients in the rock matrix that are locally orthogonal to the fracture plane (Figure 4), and neglect the effect of gradients parallel to the fracture. Hence

$$q_m = -D\frac{\partial C_m}{\partial n_b} \tag{4}$$

with D being the diffusion coefficient in the rock matrix. Note that D $[L^2T^{-1}]$ is the diffusion in pure water, D_w, multiplied by a factor $\ll 1$ which accounts for the tortuosity of the rock matrix.

In addition to the diffusive mass transfer from the flow path into the rock matrix, we consider tracer retention due to *linear equilibrium sorption*, both in the rock matrix and over the contact surface, as well as *radioactive decay*. The source term ψ_f is thereby decomposed as

$$\psi_f = \psi_f^d + \psi_f^* \tag{5}$$

where ψ_f^* is the source component due to equilibrium sorption and decay, and ψ_f^d is the rate of tracer mass transfer between the flow path and the rock matrix due to diffusion, defined as

$$\psi_f^d \equiv \frac{D\theta}{b(s)} \frac{\partial C_m}{\partial n_b} \tag{6}$$

In (6), θ is the matrix porosity assumed spatially uniform.

The source term in the fracture and the matrix are respectively written as

$$\psi_f^* \equiv -\frac{\partial C_f'}{\partial t} - \lambda C_f' \quad ; \quad \psi_m \equiv -\frac{\partial C_m'}{\partial t} - \lambda(C_\mathrm{m} + C_m') \tag{7}$$

where C_f' and C_m' are the sorbed concentrations on the contact surface, and in the rock matrix, respectively. The isotherms for equilibrium sorption are

$$C_f' = \frac{K_a}{b(s)} C_f \quad ; \quad C_m' = K_d C_m \tag{8}$$

where K_a $[L]$ and K_d [-] are the distribution coefficients on the fracture surface and in the matrix, respectively. Note that K_d is defined as $K_d = 1 + K_d'\rho_b/\theta$ where K_d' $[L^3M]$ and ρ_b $[ML^{-3}]$ is the bulk density of the rock.

Coupling equilibrium sorption with matrix diffusion, including decay, yields mass balance equations in the form

$$R_f(s)\frac{\partial C_f}{\partial t} + \frac{\partial q_f}{\partial s} = \frac{\theta D}{b(s)} \frac{\partial C_m}{\partial n_b} - \lambda R_f(s)\, C_\mathrm{f} \tag{9}$$

$$\frac{\partial C_m}{\partial t} = \frac{D}{R_m} \frac{\partial^2 C_m}{\partial n_b^2} - \lambda C_\mathrm{m} \tag{10}$$

where

$$R_f \equiv 1 + \frac{K_a}{b(s)} \quad ; \quad R_m \equiv 1 + K_d \tag{11}$$

Equations (9)-(10) are similar in form to those given, for instance, Rasmuson and Neretnieks (1984).

Next, we write (9)-(11) in terms of the mass flux following similar steps as those presented in *Cvetkovic* (1991). Substituting (3) into (9), multiplying (9) and (10) by $V(s)$, and using $s = s(\tau)$ as a transformation with $\mathrm{d}s/V(s) = \mathrm{d}\tau$, we obtain

$$R_f(\tau)\frac{\partial q_f}{\partial t} + \frac{\partial q_f}{\partial \tau} = \frac{\theta D}{b(\tau)}\frac{\partial q_m^*}{\partial n_b} - \lambda R_f(\tau)\, q_{\mathrm{f}} \tag{12}$$

$$\frac{\partial q_m^*}{\partial t} = \frac{D}{R_m}\frac{\partial^2 q_m^*}{\partial n_b^2} - \lambda R_f(\tau)\, q_{\mathrm{m}}^* \tag{13}$$

where $q_m^* \equiv C_m V$ is an auxiliary quantity. τ is the groundwater travel time from the source point ($s = 0$) to s and is computed as

$$\tau(s) = \int_0^s \frac{ds'}{V(s')} \tag{14}$$

The transformation $s = s(\tau)$ is obtained formally by inversion of $\tau(s)$, where s is now the intrinsic position of marked groundwater at time $t = \tau$. Thus the Lagrangian aperture $b(s)$, for instance, is transformed as $b(\tau) = b[s(\tau)]$, where for simplicity we use the same notation for the two functions $b(s)$ and $b(\tau)$. For $s = s_L$ where s_L is the intrinsic lenght from the canister to the biosphere, $\tau(s_L)$ is the groundwater residence time in the geosphere. Note that a Cartesian representation of the advection flow path is $\mathbf{X}(s)$ or $\mathbf{X}(\tau)$ (e.g., Dagan 1984) where the components are $\mathbf{X}(X_1, X_2, X_3)$.

4 Radionuclide discharge

The solution of (12)-(13) for specified initial and boundary conditions yields the breakthrough, or the discharge $[MT^{-1}]$ history, of a radionuclide into the biosphere (Figure 3). Any given radionuclide released at $t = 0$ and $s = 0$ at differnt geological sites, would have a different breakthrough into the biosphere; this is due to different physical and chemical properties of the site.

A simple and compact way for quantitatively characterizing the breakthrough curves in Figure 3 is by means of temporal moments. With $q_f(t, \tau)$ $[MT^{-1}]$ denoting the mass release (discharge) of a radionuclide into the biosphere where τ is the groundwater residence time from the canister to the biosphere, the "k"-th temporal moment is defined as a function of τ by

$$\int_0^\infty t^k \, q_f(t, \tau) \, dt = (-1)^k \, \frac{\partial^k \widehat{q}_f}{\partial p^k} \, |_{p=0} \tag{15}$$

where $\widehat{q}_f$ is the Laplace transform of q_f $[T^{-1}]$, and p is the Laplace transform variable.

In the following, we shall compute the temporal moments for the two scenarios, and subsequently use them for defining the GPIs.

4.1 Scenario A: Pulse release

We consider radionuclide mass m_0 released as a pulse at $t = 0$ and $s = 0$; the boundary condition is

$$q_f(0, t) = m_0 \delta(t) \tag{16}$$

Let γ $[T^{-1}]$ denote the mass discharge into the biosphere normalized by m_0, i.e. $\gamma \equiv q_f/m_0$. In Appendix A we derive $\widehat{\gamma}$ with (16) as

$$\widehat{\gamma}(p, \tau; \beta) = \exp\left[-(p + \lambda)(\tau + \beta K_a)\right] \exp\left[-\beta \, \kappa (p + \lambda)^{1/2}\right] \tag{17}$$

where $\kappa \equiv \theta \sqrt{D R_m}$, and

$$\beta(\tau) = \int_0^\tau \frac{d\tau'}{b(\tau')} \tag{18}$$

Note that using $d\tau = ds/V(s)$ and $\tau = \tau(s)$, we can write β as

$$\beta(s) = \int_0^s \frac{ds'}{V(s') b(s')} \tag{19}$$

Thus β is an integrated parameter along the advection flow path which characterizes retention due to diffusion into the rock matrix, as well as due to sorption along the contact surface. For

a simplified flow path geometry, β is the "flow wetted surface" (e.g. Moreno and Neretnieks, Olsson et al., 1995) (Appendix B).

Inversion of (17) yields the solution γ as

$$\gamma(t,\tau;\beta) = \frac{H(t-\tau)\,\beta\kappa}{2\sqrt{\pi}(t-\tau-\beta K_a)^{3/2}} \exp\left[\frac{-\beta^2\,\kappa^2}{4(t-\tau-\beta K_a)} - \lambda t\right] \tag{20}$$

where H is the Heaviside step function.

The temporal moment of order "k" are evaluated for scenario A as

$$\mu_k^{(A)}(\tau) \equiv \int_0^\infty t^k\,\gamma(t,\tau)\,dt = (-1)^k\,\frac{\partial^k\widehat{\gamma}}{\partial p^k}\,|_{p=0} \tag{21}$$

where $\widehat{\gamma}$ is the Laplace transform of γ.

From (21) and (17), the first three temporal moments for scenario A are

$$\begin{aligned}
\mu_0^{(A)} &= \exp\left[-\lambda(\tau+\beta K_a) - \beta\kappa\lambda^{1/2}\right] \\
\mu_1^{(A)} &= \mu_0^{(A)}\left[\tau + \beta\,K_a + \frac{1}{2}\,\beta\kappa\lambda^{-1/2}\right] \\
\mu_2^{(A)} &= \frac{\mu_0^{(A)}}{4}\,\beta\kappa\lambda^{-3/2} + (\mu_1^{(A)})^2/\mu_0^{(A)}
\end{aligned} \tag{22}$$

4.2 Scenario B: Continuous release

We consider total radionuclide mass m_0 released continuously at $s = 0$ at a decaying rate. The boundary condition at $s = 0$ (or $\tau = 0$) is written as

$$q_f(0,t) = q_0\,\mathrm{e}^{-\lambda t} \tag{23}$$

Let $\Gamma \equiv q_f/q_0$ [-] denote the dimensionless mass discharge into the biosphere. In Appendix A we derive $\widehat{\Gamma}$ with (23) as

$$\widehat{\Gamma}(p,\tau;\beta) = \frac{1}{p+\lambda}\exp\left[-(p+\lambda)(\tau+\beta K_a) - \beta\kappa\,(p+\lambda)^{1/2}\right] \tag{24}$$

Inversion of (24) yields

$$\Gamma(t,\tau;\beta) = \mathrm{e}^{-\lambda t}\,\mathrm{erfc}\left(\frac{\beta\kappa}{2\sqrt{t-\tau-\beta\,K_a}}\right) \tag{25}$$

The temporal moment of order "k" for scenario B is evaluated as

$$\mu_k^{(B)}(\tau) \equiv \int_0^\infty t^k\,\Gamma(t,\tau)\,dt = (-1)^k\,\frac{\partial^k\widehat{\Gamma}}{\partial p^k}\,|_{p=0} \tag{26}$$

where $\widehat{\Gamma}$ is the Laplace transform of Γ. From (15) and (24), the first three temporal moments for scenario B are

$$\begin{aligned}
\mu_0^{(B)} &= \frac{1}{\lambda} \exp\left[-\lambda(\tau + \beta K_a) - \beta\kappa\lambda^{1/2}\right] \\
\mu_1^{(B)} &= \mu_0^{(B)} \left[\lambda^{-1} + \tau + \beta K_a + \frac{1}{2}\beta\kappa\lambda^{-1/2}\right] \\
\mu_2^{(B)} &= \mu_0^{(B)} \left[\lambda^{-2} + \frac{1}{4}\beta\kappa\lambda^{-3/2} + (\mu_1^{(B)}/\mu_0^{(B)})^2\right]
\end{aligned} \tag{27}$$

5 Geosphere performance indices (GPIs)

Here we use functions γ and Γ and the temporal moments to provide quantitative definitions of specific GPIs within the three classes discussed in §2.

5.1 Containment index

The total mass released into the geosphere following scenario A or B is m_0. Let m denote the total mass of a given radionuclide released into the biosphere. The containment index (CI) is defined as the difference between the total mass released into the geosphere and biosphere, normalized with the total mass released into the geosphere:

$$CI \equiv \frac{m_0 - m}{m_0} = 1 - \frac{m}{m_0} \tag{28}$$

For scenario A, $m = \int_0^\infty \gamma dt = m_0 \mu_0^{(A)}$, whereas for scenario B, $m = q_0 \int_0^\infty \Gamma dt = q_0 \mu_0^{(B)}$. In view of $m_0 = q_0/\lambda$, the containment index (CI) is identical for scenarios A and B, and is defined by

$$CI = 1 - \exp\left[-\lambda\tau - \beta\left(K_a\lambda + \kappa\lambda^{1/2}\right)\right] \tag{29}$$

where $0 < CI < 1$. Thus CI computed for a given radionuclide and site, indicates what mass fraction would be contained by the geosphere. For instance, $CI = 0.95$ implies that 95% of radionuclide mass is contained by the geosphere by combined advection, sorption, matrix diffusion and decay. In the absence of mass transfer (i.e. retention), we have $K_a\lambda + \kappa\lambda^{1/2} = 0$, and containment depends on τ and λ only. The influence of mass transfer is contained in the parameter group $K_a\lambda + \kappa\lambda^{1/2}$ which depends both on λ and the mass transfer parameters κ and K_a.

To emphasize the dependence on the radionuclide properties, we can introduce an index "i" to designate a given radionuclide. Then the GPIs are dependent on "i". We can write the containment index CI as:

$$CI_i = 1 - \exp\left[-\lambda_i\tau - \beta\left(K_a^i + \kappa_i\,\lambda_i^{1/2}\right)\right] \tag{30}$$

and similar for other GPIs; we omit the index "i" for simplicity.

5.2 Arrival time indices

Various GPIs that provide measures of the time of arrival of a given radionuclide to the biosphere can be defined; larger values of these indices would in some sense indicate later arrival.

First, we define the *mean arrival time indices* for the two scenarios as

$$MAI(J) \equiv \left(\frac{\mu_1^{(J)}}{\mu_0^{(J)}}\right) \frac{1}{t_{M\%}} \tag{31}$$

where J=A or J=B. For instance, for J=A we get

$$MAI(A) = \frac{1}{t_{M\%}} \left[\tau + \beta \left(K_a + \frac{1}{2}\kappa\lambda^{-1/2}\right)\right] \tag{32}$$

where $t_{M\%}$ is a normalization time here suggested as

$$t_{M\%} \equiv \frac{1}{\lambda} \ln\left(\frac{100}{M\%}\right) \tag{33}$$

and $M\%$ is the percent of radionuclide mass left after time $t_{M\%}$. For instance, $t_{1\%}$ is the time required for radionuclide mass to reduce to 1% of its value at $t = 0$. Note that $t_{36.79\%} = \lambda^{-1}$. By selecting different $M\%$ (i.e. $t_{M\%}$), various stringency criteria may be employed. Thus if $M\% = 0.1\%$, then for example MAI(A)= 1.2 indicates late arrival when most of the mass has decayed, whereas MAI(A)= 0.1 indicates early arrival when little mass has decayed. If matrix diffusion iz zero (i.e. $D = 0$), then $\mu_1^{(A)}/\mu_0^{(A)} = \tau + \beta K_a$ is the retarded arrival time due to surface sorption. In the absence of surface sorption, $\mu_1^{(A)}/\mu_0^{(A)} = \tau$, i.e. the radionuclides arrive as marked groundwater; then MAI(A)= 1 implies $t_{M\%} = \tau$.

Stated in another manner, for $D = K_a = 0$ MAI(A)=1 quantifies how much mass decays during time equal to the groundwater residence time, τ; then e.g. MAI(A)=10 for $t_{1\%}$ means that groundwater residence time is 10 times larger than the time required to reduce the radionuclide mass to 1% of the released mass.

Next, we define the *fractional arrival time index* for scenario B as

$$FAI(B) \equiv t_\phi / t_{M\%} = \Gamma^{-1}(\phi, \tau; \beta)/t_{M\%} \tag{34}$$

where t_ϕ is the arrival time of a specified fraction of radionuclide release rate, ϕ, i.e. $\phi \equiv q_f(t_\phi, \tau)/q_0 = \Gamma(t_\phi, \tau)$. In (34), Γ^{-1} denotes the inverse of $\Gamma(t, \tau; \beta)$ (25). The FAI(B) can be used for defining the first-arrival, or early arrival, say as $\phi = 0.01$. Note, however, that in view of decay, Γ^{-1} will generally yield two values of t_ϕ, the early and late arrivals, depending on the chosen value of ϕ.

Finally, we define *peak arrival time indices* denoted for the two scenarios as PAI(A) and PAI(B). The arrival time of the peak is computed from γ (20), or Γ (25), by derivation with respect to t. In particular, we get for scenario A a quadratic equation in $t_p^{(A)}$

$$\frac{\partial \gamma}{\partial t} \equiv G_\gamma(t_p^{(A)}, \tau; \beta) = \lambda \left(t_p^{(A)} - \tau - \beta K_a\right)^2 + \frac{3}{2}\left(t_p^{(A)} - \tau - \beta K_a\right) - \frac{\kappa^2 \beta^2}{4} = 0 \tag{35}$$

where $t_p^{(A)}$ denotes the peak arrival time for scenario A. Similarly, for scenario B, we have

$$\frac{\partial \Gamma}{\partial t} \equiv G_\Gamma(t_p^{(B)}, \tau; \beta) = -\lambda\, e^{(-\lambda t_p^{(B)})}\, \mathrm{erfc}\left(\frac{1}{2}\frac{\beta\ \kappa}{\sqrt{t_p^{(B)} - \tau - \beta\, Ka}}\right) + \tag{36}$$

$$\frac{1}{2}\frac{e^{(-\lambda t_p^{(B)})}\, e^{\left(-\frac{1}{4}\frac{\beta^2\ \kappa^2}{t_p^{(B)} - \tau - \beta\, Ka}\right)}\ \beta\ \kappa}{\sqrt{\pi}\,(t_p^{(B)} - \tau - \beta\, Ka)^{3/2}} = 0$$

Both $t_p^{(A)}$ and $t_p^{(B)}$ are generally obtained in an implicit form. Using $t_p^{(J)}$, J=A,B, we define the peak arrival indices as

$$PAI(J) \equiv \frac{t_p^{(J)}}{t_{M\%}} \tag{37}$$

5.3 Dilution indices

The purpose of dilution indices is to provide effective measures of the potential dilution due to mass transfer reactions; these indices can be defined in various ways. The dilution is minimum if the entire radionuclide mass m_0 arrives to the biosphere as a pulse, i.e. over a short period of time, which would happen in the absence of hydrodynamic dispersion and mass transfer. Thus one way to quantify dilution for a given radionuclide and site is to compute the time during which radionuclide mass would be discharged into the biosphere. Larger values would imply longer times over which radionuclides are discharged and hence greater dilution, and *vice versa*. Another indicator of dilution is the peak of the discharge. In particular, for minimum dilution, the peak is maximum for pulse release and arrival; thus a decreasing peak implies increasing dilution effects.

We first use the second central moment of the breakthrough to define the *dilution indices* for the two scenarios as

$$DI(J) \equiv \frac{1}{t_{M\%}}\sqrt{\frac{\mu_2^{(J)}}{\mu_0^{(J)}} - \left(\frac{\mu_1^{(J)}}{\mu_0^{(J)}}\right)^2} \tag{38}$$

where J=A or J=B. For example, for J=A, we have

$$DI(A) = \beta^{1/2}\left(\frac{\kappa^{1/2}\lambda^{-3/4}}{2t_{M\%}}\right) \tag{39}$$

An alternative definition for the scenario B could have been provided using the fractional arrival time. In particular, the difference between the two values of t_ϕ obtained from Γ^{-1}, the early and late arrival times.

Next, we use the peak value of either γ or Γ as a measure of dilution. First the peak arrival times, $t_p^{(J)}$, J=A,B, need to be computed as functions of τ, β and other parameters as described in §5.2; the peak values of γ and Γ can then be evaluated by substituting $t_p^{(J)}$, J=A,B, into γ and Γ. For example, $t_p^{(B)}$ is obtained in an implicit form from $\frac{\partial \Gamma}{\partial t} \equiv G_\Gamma(t_p^{(B)}, \tau; \beta) = 0$. Solving $G_\Gamma = 0$, we obtain $t_p^{(B)} = t_p^{(B)}(\tau, \beta)$ which is then substituted into Γ to yield the peak discharge, wherefrom we define the *peak index* as

$$PI(B) \equiv \Gamma\left[t_p^{(B)}(\tau, \beta), \tau, \beta\right] \tag{40}$$

Thus PI(B) is a function of τ, β and of the remaining parameters.

5.4 Controlling parameters

All the defined GPIs depend on the following five parameters: $\lambda, \kappa, K_a, \tau$ and β. The parameter λ is intrinsic to a given radionuclide. The parameter K_a and the parameter group $\kappa = \theta\sqrt{DR_m}$, depend on the combined physical-chemical properties of the rock matrix and a given radionuclide, and in principle can be measured in the laboratory from rock samples.

The parameters τ and β are associated with flow and advective transport through fractures. In particular, β is dependent on the variable aperture of fractures, and on the flow. Both τ and β are field-scale parameters that can be determined only from field-scale information.

6 Statistical formulation of GPIs

The quantities τ and β are random due to natural heterogeneity of geological media. At best, τ and β can be described statistically, by a joint probability density function (PDF) $f(\tau, \beta; \mathcal{L})$ where $\mathcal{L}$ denotes the surface between the geosphere and biosphere; $f(\tau, \beta; \mathcal{L})$ needs to be determined for a given site based on sampled data. In our following discussion we shall assume that the joint PDF $f(\tau, \beta; \mathcal{L})$ has been determined by a combination of field measurements and numerical simulations.

Due to the randomness of τ and β, the GPIs are random. In fact, all the GPIs defined in §7 should be viewed as conditioned on particular values of τ and β.

Our task in this Section is to derive PDFs of the GPIs given the joint PDF $f(\tau, \beta; \mathcal{L})$.

The general form of the GPIs is

$$GPI = a\,\delta$$

where a is a constant, and δ is a random quantity given in an implicit form as a function of β and τ as $G(\delta, \tau, \beta) = 0$. For instance, for FAI(B) defined in (34), $a \equiv 1/t_{M\%}$ and $\delta \equiv t_\phi$; also, $G \equiv \phi - \Gamma(t_\phi, \tau; \beta) = 0$.

Using the general result of Appendix B, we derive the PDF of δ as

$$f(\delta) = \int_0^\infty f_{\tau\beta}[\tau, \beta(\delta, \tau)] \left| -\frac{\partial G/\partial \delta}{\partial G/\partial \beta} \right| d\tau \tag{41}$$

where $\beta > 0$ provides a constraint on the integration interval for τ, and $f_{\tau\beta}$ is the joint PDF for τ and β. Once $f(\delta)$ is computed, the PDF for the GPI is

$$f(GPI) = \frac{1}{a} f\left(\frac{GPI}{a}\right) \tag{42}$$

wherefrom we readily compute the cumulative distribution. The major computational effort in determining $f(GPI)$ is obtaining $\beta = \beta(\delta, \tau)$ from the implicit form $G(\delta, \tau, \beta) = 0$.

The corresponding probabilities for any GPI are computed as

$$F(GPI) = \int_0^{GPI} f(g)\, dg \tag{43}$$

where f is the PDF of any GPI.

7 Illustration examples

The simplest expressions of the PDFs are obtained for the containment index CI, the arrival time index MAI(A), and the dilution index DI(A); we illustrate these in the following. In all cases, we identify the mean groundwater residence time, $E(\tau)$, as the characteristic time, denoted by $T \equiv E(\tau)$ [T], and use it as a normalization parameter. Similarly, we identify the mean of β, $E(\beta)$, as the characteristic β, denoted by $B \equiv E(\beta)$ [TL^{-1}], and use it as a normalization parameter.

7.1 Containment index

The PDF for CI is the special case (56) and reads

$$f[CI] = \frac{1}{e(1-CI)} \int_0^{\tau^*} f_{\tau\beta} \left[\tau, \frac{\ln[(1-CI)^{-1}] - \lambda\tau}{e} \right] d\tau \tag{44}$$

where $e \equiv \lambda K_a + \kappa\lambda^{1/2}$, and $\tau^* = (1/\lambda)\ln[(1-CI)^{-1}]$ in view of $\beta > 0$.

In Figure 4 we illustrate a few type curves of the probability of the containment index, $F(CI)$, obtained by integrating $f[CI]$ (44). The curves of Figures 4 illustrate the effect of the deterministic parameters λ and $e = \lambda K_a + \kappa\lambda^{1/2}$, as well as of the statistical parameters of τ and β. We assume a joint-lognormal PDF for τ, β where the moments $E(\tau)/T = 1$, $E(\beta)/B = 1$, $CV(\tau) \equiv SD(\tau)/T$ $CV(\beta) \equiv SD(\beta)/B$, and the correlation coefficient $\rho \equiv COV(\tau\beta)/[SD(\tau)SD(\beta)]$ are the input statistics; $SD(\cdot)$ denotes the standard deviation of a given quantity and $COV(\cdot)$ the covariance function. Thus the variability is quantified by the coefficients of variation $CV(\tau)$ and $CV(\beta)$, which we assume for simplicity as equal, i.e., $CV \equiv CV(\tau) = CV(\beta)$; in all the computations, the correlation coefficient ρ is assumed 0.7. The dimensionless deterministic parameters are λT and eB; for simplicity, we use in the following the notation λ and e for dimensionless values, λT and eB.

In Figure 4a we assume a relatively low variability with $CV = 0.2$, whereas in Figure 4b we assume a higher variability with $CV = 0.7$. All the curves in the two figures show a similar pattern, with the form of the probability curves being different. For small λ and e, the CI is small, in the limit being zero. As λ and e increase, the curves shift toward increasing CI, such that for the largest values considered, the probability is one for the value of CI close to unity, i.e., the entire radionuclide mass is contained by the geosphere with probability one. The parameter e incorporates the effect of both mass transfer and decay, and thus can be viewed as critical. Small λ implies slow decay and hence less chance of containment. However, if e is of the order 1 or larger, containment will be substantial even if λ is small. This is because

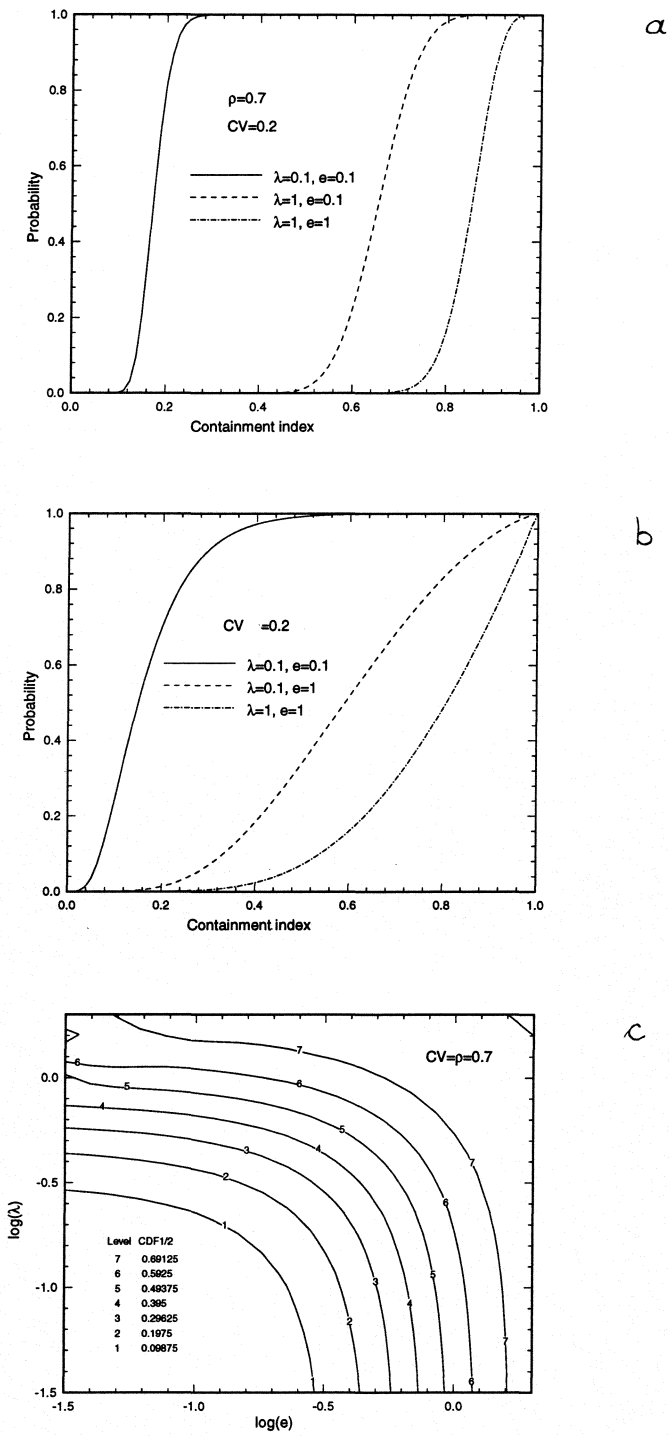

Figure 4: Probability of the containment index for scenario (A) (CI(A)), (a) for a set of dimensionless parameters λ and e with CV=0.2, (b) for a set of dimensionless parameters λ and e with CV=0.7, (c) as a surface plot in the dimensionless log-parameter space with CV=0.7 ; in all cases, the correlation coefficient, ρ, is set as 0.7.

with λ small, e of the order 1 implies large retention that is controlled by K_a and κ. Note that the curves for $\lambda = 0.1$, $e = 1.0$ and $\lambda = 1.0$, $e = 0.1$ are identical, i.e. there is symetrical influence of the two parameters λ and e.

Figure 4c illustrates the probability of the containment index being equal or less 1/2, in the log-parameter space, $\log(\lambda)$ and $\log(e)$. The value provided by the isolines was obtained by reading the probability at CI(A)=1/2 in Figure 4b and subtracting it from 1. This yields the probability of CI(A)>1/2 which was chosen as indicative of a high containment index. The probability of the containment index >1/2 is dispersed in the log-parameter space due to the heterogeneity and resulting uncertainty in τ and β. The isoline labled 1 in Figure 4c provides a limit of approximately 10% probability, indicating that for the parameter values as low as $\log(\lambda) < -0.5$ and $\log(e) < -0.5$, the probability that the containment index can be $> 1/2$ is small (10%) Similarly, for $\log(\lambda) > 0.2$ and $\log(e) > 0.2$, the probability is 70% that the containment will be >1/2. Note that in the deterministic case, a single curve (i.e. a sharp front) separates the zone where the containment index is $< 1/2$ from the zone where the containment index is >1/2.

7.2 Mean arrival time index

The PDF for MAI(A) is

$$f[MAI(A)] = \frac{1}{a}\int_0^{\tau^*} f_{\tau\beta}\left(\tau, \frac{MAI(A) - \tau/t_{M\%}}{a}\right) d\tau \tag{45}$$

where $a \equiv \left(K_a + 12\kappa\lambda^{-1/2}\right)/2t_{M\%}$ and $\tau^* = MAI(A)t_{M\%}$. We normalize the parameter a as aB, and illustrate the dependence of the probability (i.e. cumulative f(MAI)), on the system parameters.

As before, we fix the correlation coefficient as $\rho = 0.7$, and show curves for $CV = 0.2$ (Figure 5a) and for $CV = 0.7$ (Figure 5b), for combinations of dimensionless λ and a. In both Figures, we set M%=0.1%, whereby the mean arrival time is normalized with the time required for the radionuclide mass to decay to 0.1% of its original mass. Thus a value of MAI close to 1 indicates a mean arrival time that is of the same order as the time required for 99.9% mass to decay. Higer values of MAI are more favourable from the safety standpoint, and *vice versa*. The strong influence of the retention parameter a is apparent. For large a, the tracer is considerably more delayed than for the lower value (0.1). The influence of variability is again to disperse the probability curve. The dispersion of the probability curve also depends on λ, being larger for increasing λ. Note that the curves could have been plotted for values of MAI(A) larger than 1.

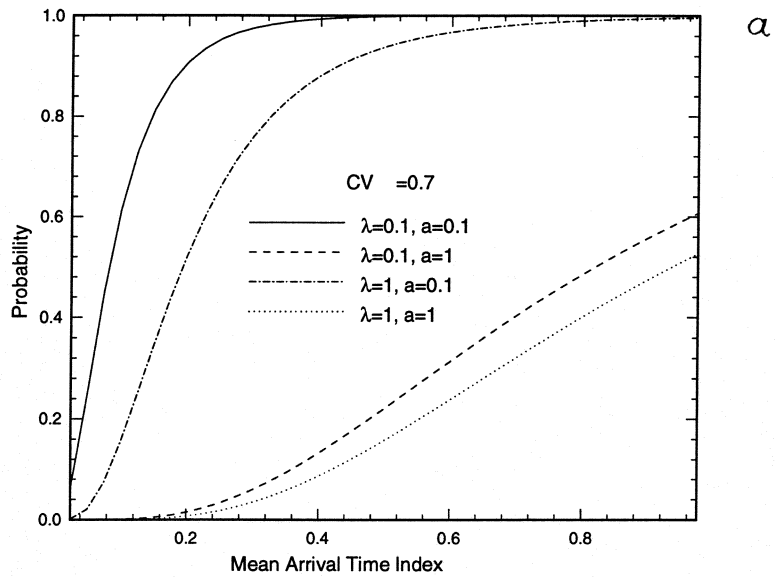

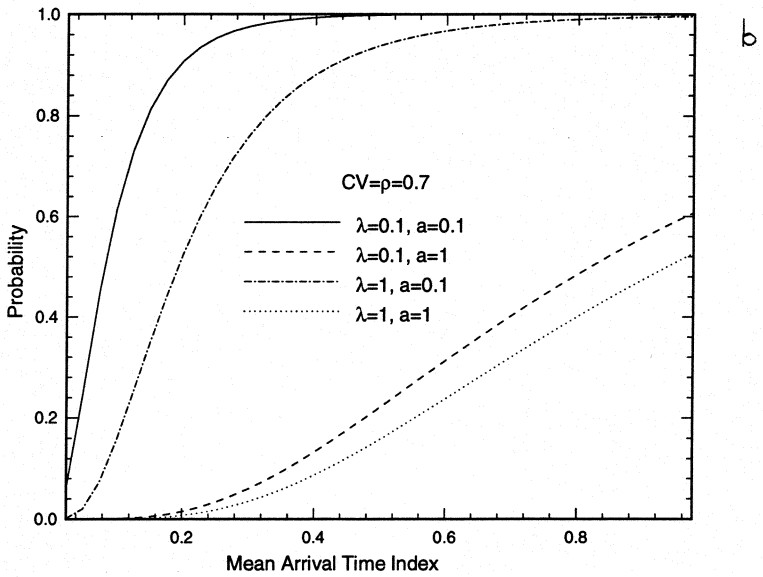

Figure 5: Probability of the mean arrival time index for scenario (A) (MAI(A)), for a set of dimensionless parameter values λ and a, for (a) CV=0.2, (b) CV=0.7; in both cases, the correlation coefficient, ρ, is set as 0.7.

7.3 Dilution index

The PDF for the DI(A) is

$$f[DI(A)] = \frac{2DI(A)}{d^2} \int_0^\infty f_{\tau\beta}\left(\tau, \frac{DI(A)^2}{d^2}\right) d\tau \tag{46}$$

where $d \equiv \theta^{1/2}(DR_m\lambda^{-3})^{1/4}/2t_{M\%}$. Note that DI(A) depends only on one deterministic parameter group, d. We normalize d as $dB^{1/2}T^{-1}$.

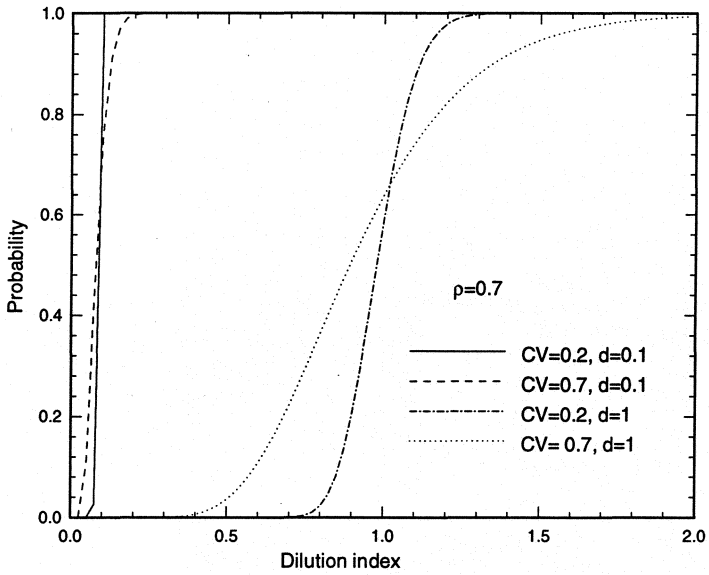

Figure 6: Probability of the dilution index for scenario (A) (DI(A)), for a set of dimensionless parameter values d, and for different values of the CV; in all cases, the correlation coefficient, ρ, is set as 0.7.

In Figure 6, we illustrate the probability for the dilution index for a few combinations of dimensionless d and CV. Again, the correlation coefficient is 0.7 and we set M%=0.1%. The dilution index is strongly affected by the value of d. For low d, DI(A) is relatively small (<0.2), with probability 1 even for large uncertainty (CV=0.7). Thus the effect of uncertainty on DI(A) depends largerly on the retention-decay parameter, d. A large DI(A) is favourable from the safety assessment standpoint.

8 Summary

In this document we propose the concept of *Geosphere Performance Indices* (GPIs); the "performance" refers to the geosphere's capacity to retain/contain radionuclides in the event of their accidental release at some point in time. The GPIs are based on the Lagrangian stochastic-analytical framework for transport in the subsurface and are believed to render useful tools in performance assessment studies in general and in the site selection process in particular. Furthermore, the use GPIs is consistent with the regulatory demands for clear factors and criteria used in the site selection process.

A main advantage of the GPIs is their transparency and low computational effort. Furthermore, additional data in a site selection programme is easily incorporated into the GPIs in an iterative manner; only the PDFs have to be updated. In the provided illustration examples analytical PDFs have been assumed; however, it is emphasized that in a real application the PDFs most likely will be obtained through combined data acqusition in the field/lab and numerical simulations. The simulations will only imply conservative transport and aperture registration along flowpaths since all mass transfer calculations are implicitely contained in the formulation of the GPIs; thus the computational effort can remain at a relatively low level even for complex hydrogeological sites.

The illustrated probability curves for a few GPIs are simple: The numbers are dimensionless and essentially range from 0 to 1. For each site and radionulcide, every GPI would result in a curve of the type illustrated in Figures 4-6. These curves are convenient to compare between different sites. The curves depend on site-specific parameters (e.g. sorption properties, matrix porosity, diffusivity) and field-scale properties summarized as statistical parameters of τ and β. As illustration figures indicate, the probability of the GPIs depend strongly on the dimensionless system parameters eB, aB and $dB^{1/2}T^{-1}$. Thus it is important to estimate correctly not only the deterministic parameters e, a and d, but also the mean values of β and τ, B and T, respectively. The exact degree of correlation between τ and β seems less important. The degree of uncertainty due to heterogeneity that is expressed by the $CV(\tau)$ and $CV(\beta)$ is important for the shape of the probability curves, although the curves do not appear too sensitive to the exact value of the CVs.

It is proposed that the derived framework is further elaborated and applied for realistic geosphere cases. This may either be done by simulating generic but plausible random fields of the geosphere in 3D using continuum or discrete approaches. Alternatively, existing field data (e.g. Finnsjön and/or Äspö) could be used in conjunction with numerical simulations conditional to the field data in order to provide indications of geosphere performance at sites

previously used in a safety assessement context. A main issue in both the generic and site-specific analyses would be to investigate in a comprehensive manner the sensitivity of the GPIs on the underlying parameters and their statistical distributions.

The methodology outlined in this report is based on the same conceptual framework as used in the prediction and evaluation exercise of reactive tracer tests within the TRUE undertaking at the Äspö Hard Rock Laboratory (Cvetkovic et al., submitted; Cvetkovic et al., in preparation). This may be seen as a safeguard that the GPIs are formulated on the most current and state-of-the-art understanding of transport and mass transfer processes in fractured rock. The parallel use of the proposed conceptual framework for characterization and site selection, guarantees that the field data fed into GPIs actually is measurable using standard field-scale hydraulic and tracer test techniques. Also, a recently developed analytical model for relating the statistics of τ and β to the statistics of fracture networks (Painter et al., in press) can find its direct use in computing the probability of GPIs.

9 Appendix A: Laplace transform solutions

Initially, both the fracture and the matrix are free from radionuclides; hence $C_f(s,0) = C_m(s,0) = 0$, or after multiplication by the fluid velocity V,

$$q_f(s,0) = q_m^*(s,0) = 0 \tag{47}$$

Furthermore, we assume the matrix to be large (unbounded). An additional condition is $C_f = C_m$ for $n_b = 0$, or after multiplication by V,

$$q_f = q_m^* \qquad \text{for} \qquad n_b = 0 \tag{48}$$

where C_f (i.e., q_f) is independent of s.

Taking the Laplace transform of (12), (13), and (48), a system of equations in the Laplace domain is obtained as

$$R_f(s)\widehat{q}_f(p+\lambda) + \frac{d\widehat{q}_f}{d\tau} = \frac{\theta D}{b(s)}\frac{d\widehat{q}_m^*}{dn_b} \qquad \text{for} \qquad n_b = 0, \qquad s > 0 \tag{49}$$

$$\frac{d^2\widehat{q}_m^*}{dn_b^2} - \frac{(p+\lambda)R_m}{D}\widehat{q}_m^* = 0 \qquad \text{for} \qquad n_b > 0 \quad , \quad s > 0 \tag{50}$$

$$\widehat{q}_f = \widehat{q}_m^* \qquad \text{for} \qquad n_b = 0 \tag{51}$$

where the circumflex denotes the Laplace transform and p is the Laplace transform variable. Note that the dependence on s in (51) can be substituted for the dependence on τ using the transformation $s(\tau)$ obtained by inverting $\tau(s)$.

The solution of (48) with (51) is $\widehat{q}_m^* = \widehat{q}_f \exp\left\{-\left[(p+\lambda)R_m/D\right]^{1/2} n_b\right\}$ whereby (47) reduces to

$$\frac{d\widehat{q}_f}{d\tau} = -\left[R_f(s)(p+\lambda) + \frac{\kappa(p+\lambda)^{1/2}}{b(s)}\right]\widehat{q}_f \tag{52}$$

The transformed boundary and initial conditions are

$$\widehat{q}_f = m_0 \qquad \text{for} \qquad s = 0$$

$$\widehat{q}_m^* \qquad \text{finite as} \qquad n_b \to \infty \tag{53}$$

$$\widehat{q}_m^* \quad \text{and} \quad \widehat{q}_f \quad \text{finite as} \quad s \to \infty$$

Integration of (52) with (53) and division by m_0, yields (20).

10 Appendix B: A few results from probability theory

Let $f(x, y)$ denote a joint PDF of x and y. Consider the transformation $u = u(x, y)$ and $v = v(x, y)$. The joint PDF $f(u, v)$ is evaluated as

$$f(u, v) = \mid J \mid f_{xy}[x(u, v), y(u, v)] \tag{54}$$

where the inverse transformation is $x = x(u, v)$ and $y = y(u, v)$, and the subscripts on f_{xy} emphasize the joint PDF of x and y. In (54), J is the Jacobian defined as the determinant of the matrix

$$J = \frac{\partial[x, y]}{\partial[u, v]}$$

The marginal PDF $f(u)$ is obtained as $f(u) = \int f(u, v)\, dv$. Now consider the particular transformation $u = u(x, y)$ and $v = x$. Then

$$f(u) = \int f_{xy}[x, y(u, x)] \mid J \mid dx \tag{55}$$

where $J = dy/du$. If $u = u(x, y)$ is given in an implicit form, e.g., $G(u, x, y) = 0$, then $J = -(\partial G/\partial u)(\partial G/\partial y)$; $y(x, u)$ in (55) has to be computed from $G(u, x, y) = 0$.

A special case is if $u = x + y$. Then $J = 1$ and the PDF $f(u)$ is computed as

$$f(u) = \int f_{xy}(x, u - x)\, dx \tag{56}$$

Another special case is if $u = u(y)$ and $v = x$, then we recover

$$f(u) = f_y[y(u)] \mid dy/du \mid \tag{57}$$

References

Andersson, J., et al., Parametrar av betydelse att bestämma vid geovetenskaplig platsundersökning, SKB R-97-03, 1997.

Cvetkovic, V., J. O. Selroos and H. Cheng, Transport of reactive tracers in rock fractures, submitted

Cvetkovic, V., J. O. Selroos and H. Cheng, Evaluation of TRUE-1 experiments at Äspö: Theory and applications, in preparation.

Moreno, L., and I. Neretnieks, Flow and nuclide transport in fractured media: The importance of the flow-wetted surface, J. Contam. Hydrology, 13, 49-71, 1993.

Miljödepartmentet, Regeringsbeslut 25, 1996-12-19, 1996.

Olsson, O., Äspö Task Force on Modelling of Groundwater Flow and Transport of Solutes, Issue Evaluation Table, SKB ICR 95-06, SKB, 1995.

Olsson, O., Neretnieks, I., and Cvetkovic, V., 1995. Deliberations on radionuclide transport and rationale for tracer transport experiments to be performed at Äspö - a selection of papers, SKB Äspö Progress Report 25-95-01.

Painter, S., V. Cvetkovic, and J.O. Selroos, Transport and retention in fractured rock: Consequences of a power-law distribution for fracture lengths, *Physical Reviews E* 57, 6917-6922, 1998.

Rasmuson, A., and I. Neretnieks, Radionuclide transport in fast channels in crystalline rock, Water Resour. Res., 22, 1247-1258, 1984.

Selroos, J.-O., 1997a. A stochastic-analytical framework for safety assessment of waste repositories: 1. Theory, Ground Water, vol. 35, No. 3, pp. 468-477.

Selroos, J.-O., 1997b. A stochastic-analytical framework for safety assessment of waste repositories: 2. Application, Ground Water, vol. 35, No. 5, pp. 775-785.

SKB, Översiksstudie 95, Lokalisering av djupförvar för använt kärnbränsle, SKB,1995.

SKI, SKIs utvärdering av SKBs FUD-Program 95, Gransknings-PM, SKI Rapport 96:48, SKI, 1996.

Vieno, T., A. Hautojärvi, L. Koskinen, and H. Nordman, TVO-92 Safety analysis of spent fuel disposal, Report YJT-92-33 E, YJT, Helsinki, Finland, 1992.